PAPER • **OPEN ACCESS**

Analysis of oxide scales on oxidised EN 1.4509 ferritic stainless steel catalyst support by scanning electron microscopy

To cite this article: P Navarro Vicente *et al* 2020 *IOP Conf. Ser.: Mater. Sci. Eng.* **891** 012017

IOP Conf. Series: Materials Science and Engineering **891** (2020) 012017 doi:10.1088/1757-899X/891/1/012017

Analysis of oxide scales on oxidised EN 1.4509 ferritic stainless steel catalyst support by scanning electron microscopy

P Navarro Vicente[1], A Nuñez Galindo[1], J F Almagro Bello[1] and J A Odriozola[2]

[1] Acerinox Europa S.A.U, Departamento Técnico / Laboratorios e Investigación, Pol. Industrial Palmones s/n, 11379 Los Barrios, Spain
[2] CSIC-Universidad de Sevilla, Instituto de Ciencia de Materiales de Sevilla, Avda. Americo Vespucio 49, 41092 Seville, Spain

E-mail: pablo.navarro@acerinox.com

Abstract. This study aims to investigate the oxidation behaviour at high temperature of a commercial ferritic stainless steel EN 1.4509. Tests of high temperature oxidation in air were carried out under isothermal condition (950 ºC) with different exposure times in order to obtain the oxidation kinetics law associated to this material. The surface and cross-section were analysed by scanning electron microscopy and energy-dispersive X-ray spectrometry (SEM/EDS), where the oxide scales proved to be formed by an external Mn-Cr spinel and an inner chromia layer. These oxides were generated by the migration of metallic cations from the stainless steel to the atmosphere. The size of the generated spinel crystals increased when increasing the exposure time as well as the cross-section thickness did. Moreover, the surface modification of ferritic stainless steel EN1.4509 was studied when platinum is deposited on its surface. The feature of this surface-modified ferritic stainless steel against oxidative atmosphere was evaluated by SEM/EDS. This platinum deposition led to reach a different surface morphology in terms of crystal size and nature.

1. Background

The use of metallic structured catalytical reactors has attracted a great deal of attention as alternative to traditional catalyst [1]. These structures have been manufactured with different metals and alloys. Among the different substrate material reported, the thermal stability and the mechanical shock resistance properties is a key advantage of manufacture stainless steel structured support [2].

From a thermodynamic point of view, the oxidation reaction in metals is explained using the following reaction:

$$M\,(s) + n\,\frac{1}{2}\,O2 \rightarrow MOn\,(s) \qquad (1)$$

This reaction occurs when the free energy of the system is $\Delta G^{o} \leq 0$ [8]. The oxidation is a reaction between oxygen and metallic elements in the metal-gas interphase which produces an oxide. At a high temperature, the oxidation in metals produces a thick oxide whose growth will obey parabolic time

dependence. This consideration was first described by Wagner. According to this theory, the growth takes place by the inward transport of ions [3]. The oxide scale is inhomogeneous. The two major potential phases in a ferritic stainless steel oxide scale are the chromia and Mn-Cr spinel [4].

The main aim of this work is the characterization of a commercial ferritic stainless steel EN 1.4509 used as a catalytic support under oxidative atmosphere. In the field of catalysis, when stainless steel is used as a support, it undergoes thermal treatment in order to generate an oxide scale that improves the anchoring and the deposition of the active phase [5].

The evaluation of the oxide scales formed during the thermal treatment at different exposure times provides information about the migration processes that are taking place. Surface and cross-section samples have been evaluated using scanning electron microscopy and energy-dispersive X-ray spectrometry (SEM/EDS) in order to study the changes in the topography and chemical composition of the phases during oxidation. The deposition of platinum on ferritic stainless steel is also studied for the comparison of the impact of noble metals during the oxidation reaction.

2. Experimental and discussion

2.1. Material selected

The selected material is a commercial ferritic stainless steel EN 1.4509 supplied by Acerinox Europa S.A.U. (1 mm thick). Prior to thermal treatment, samples were cut in 30 cm × 30 mm. The chemical composition of the material is shown in Table 1. All elements were analysed by X-ray fluorescence using a Panalytical PW 2606 XRF spectrometer, except for C and N, which were analysed by Leco CS 600 and TC 600 analysers, respectively.

Table 1. Elemental composition of stainless steel EN 1.4509.

Element	Al	C	Cr	Cu	Mn	Mo	N	Nb	Si	Ti
at%	0.045	0.021	17.525	0.123	0.347	0.019	0.019	0.386	0.401	0.122

2.2. Thermogravimetric experiments

The weight-gain curve, as a function of time for the ferritic material EN 1.4509 after being oxidised in air at 950 ºC is shown in

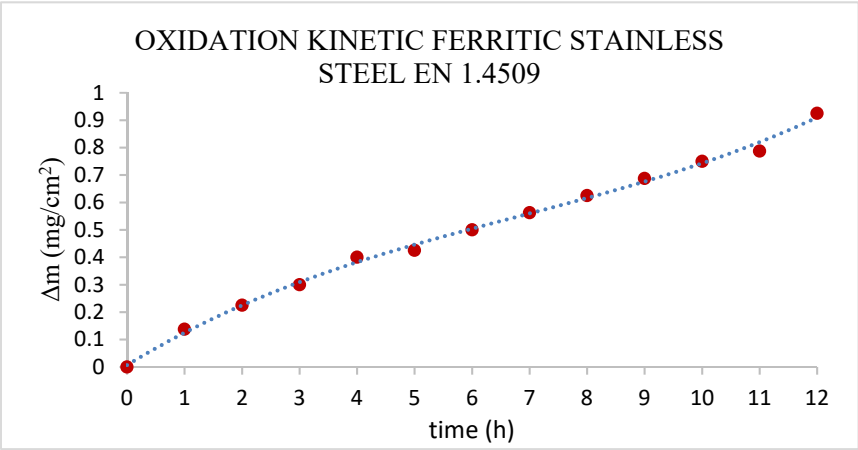

Figure 1. Mass change versus time curve for EN 1.4509 ferritic stainless steel oxidized in air for 12 hours.

The sample weight gradually increases as a function of time. The results show how the points are fitted to a parabolic curve. This kinetic behaviour indicates that the growth is controlled by the inward transport of metal cations of the substrate and/or the inward anions transport from the gas [6]. This suggest that during the early stages of the thermal treatment, the oxide layer is growing rapidly by the outward migration of the elements, but when this layer has a critical thickness, the transport is blocked, and the growing rate is reduced [7].

2.3. Microstructural evaluation

The characterisation was performed on a Zeiss ULTRA 55 FEG-SEM. Backscattered electron (BSE) images were analysed at an accelerating voltage of 10 kV and a working distance of 8.5 mm. For the purpose of investigating the morphological modifications during the oxidation process, the specimens tested under different thermal treatment are shown in Fig. 2.

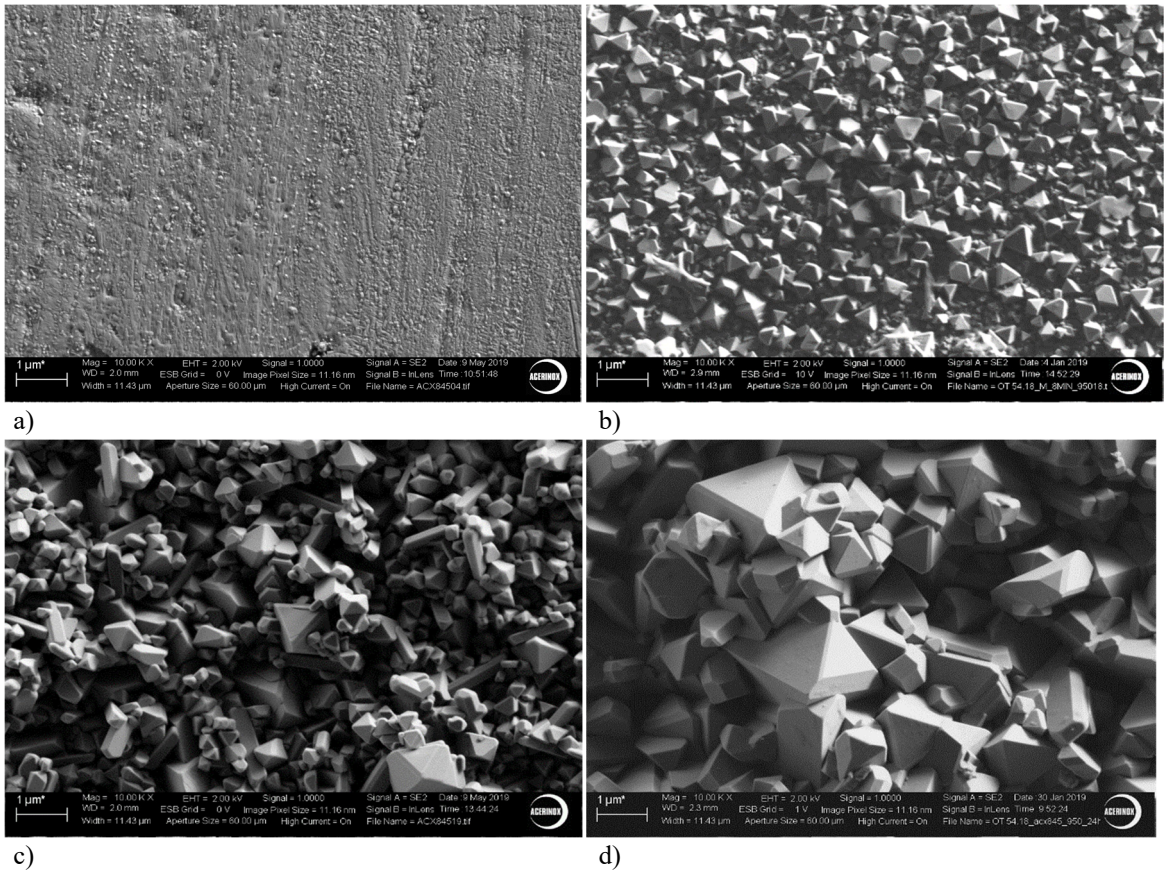

Figure 2. Surface morphology of the ferritic stainless steel EN 1.4509: a) Untreated; and thermal treated at 950 ºC in air for b) 8 min; c) 24 hours, and d) 168 hours.

Figure 2a shows thee morphology of the ferritic stainless EN 1.4509 before any thermal treatment. A modified surface was observed in Fig. 2b after a thermal treatment for 8 min at 950 ºC. This modification is attributed to the migration of metals to the surface and the formation of a crystal phase. It should be noted that surface is not completely covered by these crystals. A different topography is found after 24 hours test in for this sample, the crystal size has increased and the surface is entirely coated. A similar situation is observed in Fig. 2d. If the sample is heated in a long thermal treatment of 168 hours, an increase in the crystal size is also noted.

In all samples, regardless thermal treatment time, the oxidation products grows in an octahedral shape which is associated to stainless steel spinels in the literature [8]. Table 2 shows the EDS point analysis composition of the oxides products corresponds to a sample heated during 24 h at 950 ºC. All analyses were performed at an accelerating voltage of 10 kV.

Table 2. Chemical composition from EDS point analysis for crystals formed (in at%).

Sputtering	Phase	O	Al	Si	Ti	Cr	Mn	Fe	Nb
No	spinel	57.57	0.17	0.19	0.48	23.34	15.75	2.40	0.10
Yes	spinel	57.56	0.31	0.03	0.28	26.31	13.69	1.82	0
Yes	chromia	59.58	0.18	0.02	0.29	36.45	2.84	0.64	0

According to the chemical composition and the structure, this oxidation product is attributed to Mn-Cr spinel phase, with some contribution from other elements.

The spinel layer observed on the oxidized samples correspond to the most external one of the studied oxide scale. The spinel phase grow over a chromia protective layer. The Cr_2O_3 is not stable at high temperature and its volatilisation takes place thermodynamically [9]. However, the spinel layer formed over the chromia has a key role in the thermal behaviour of the material, inhibiting effectively the diffusion of chromium to the atmosphere [10].

Samples were prepared for FEG-SEM cross-section observation. A comparison between the cross-section of the heated samples is displayed in Figure 3. The BSE image reveals the variation of the oxide scale thickness generated during the oxidation process at different exposure time.

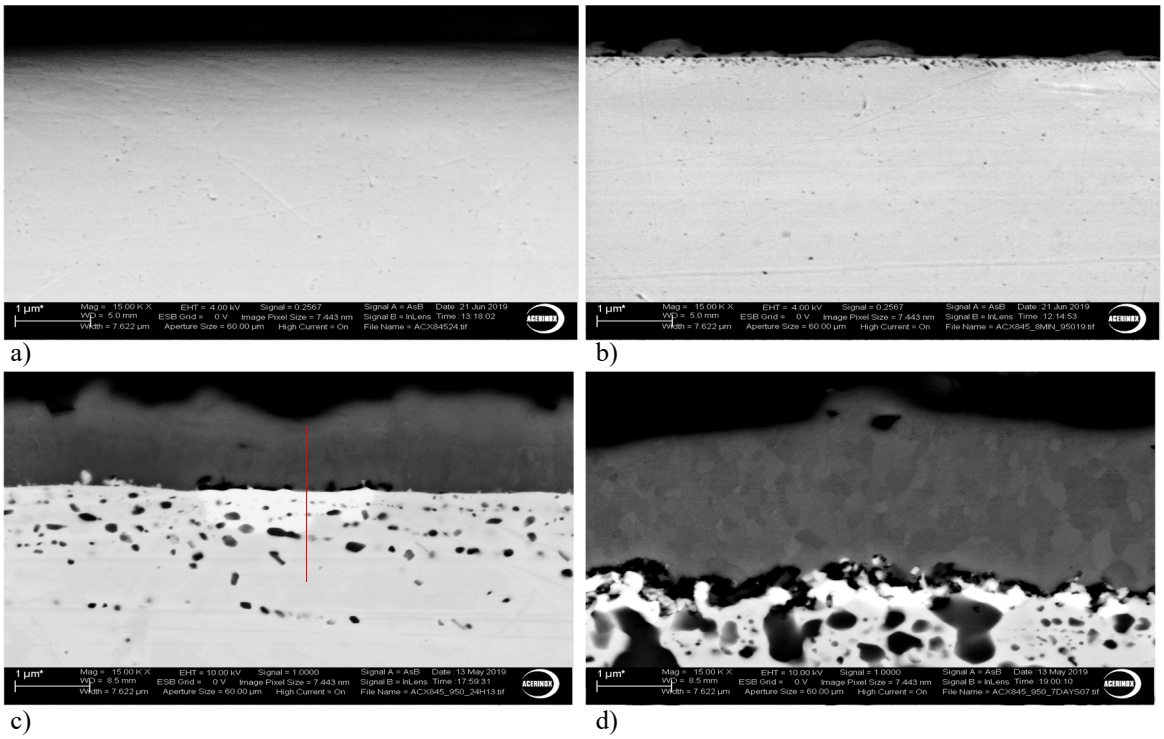

Figure 3. Cross-section view of the ferritic stainless steel EN 1.4509. a) Untreated. Thermal treated for: b) 8 min; b) 24 h; and d) 168 h.

Figure 3a is the untreated EN 1.4509 stainless steel. This sample does not exhibit any oxide scale, however, after 8 minutes at 950 ºC, a thin oxide scale over the surface of the stainless steel can be appreciated in Figure 3b. When the exposure time raise 24 hours in the Figure 3c, due to the long diffusion time, the thickness of the oxide increase its size. Also is noted that the oxide scale is formed by two layers: an external spinel phase and an inner chromia protective layer [11]. As a result of the inward migration of oxygen, internal oxides were formed below the interphase oxide scale/stainless steel. According to literature, the white phase in the image is attributed to the intermetallic precipitation. A long term test of 168 hours, as shown Figure 3d, reveals that the oxide scale remains growing with the exposure time. The massive element migration has altered the interphase oxide scale/stainless steel, and due to the prolonged inward diffusion of the oxygen, the size and proximity of the internal oxides were increased. This prolonged oxidation test seems to generates an intermetallic continuous barrier.

2.4. Chemical analysis

The element migration during the thermal treatment was evaluated by energy-dispersive X-ray spectrometry (EDS). EDS mapping analysis in the cross-section of the oxidised specimens for 8-minute and 24-hour periods are shown in Figs. 4 and 5, respectively. The distribution and composition of the elements after testing show the influence of oxidation exposure time.

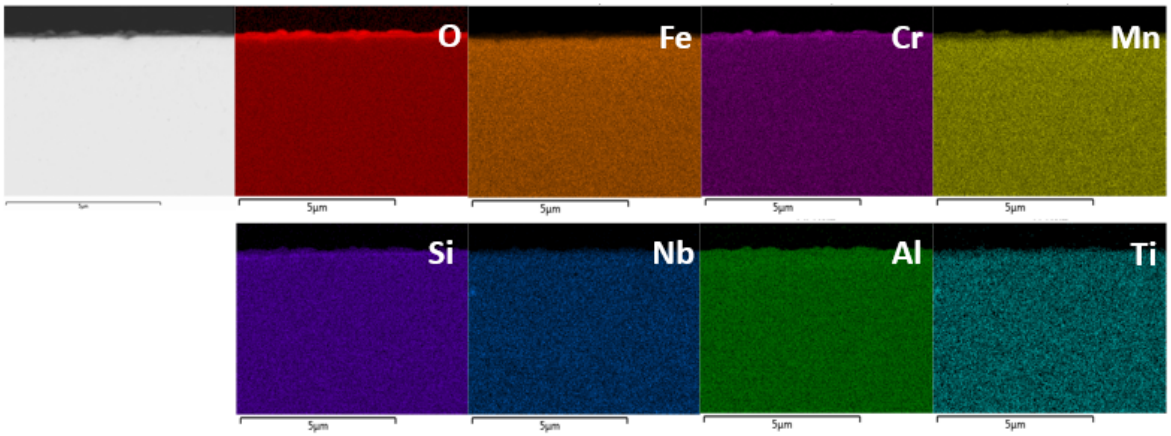

Figure 4. EDS elemental mapping of the specimen oxidised 8 min. at 950 °C.

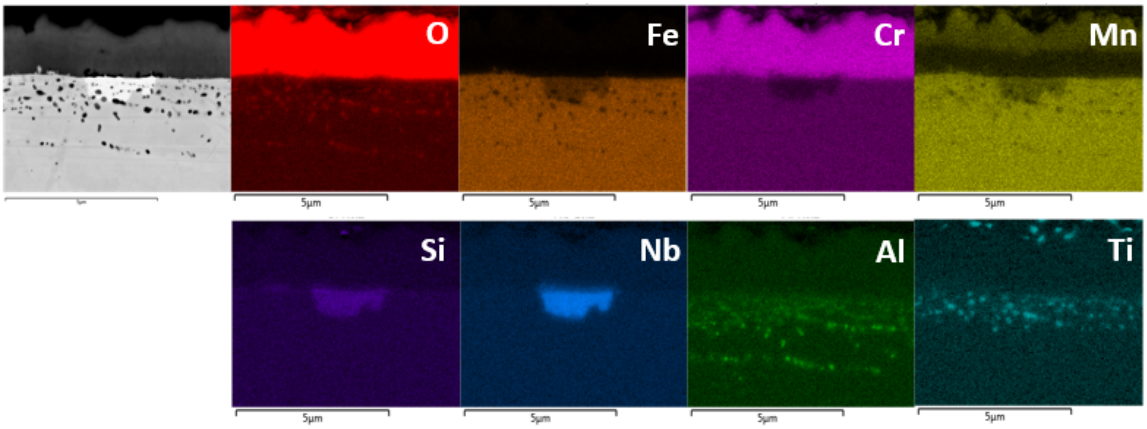

Figure 5. EDS elemental mapping of the specimen oxidised 24 h at 950 ºC.

As shown in Fig. 4, oxygen is only concentrated in the most external layer of the sample, indicating the absorption in the surface, forming the protective chromia layer (with Cr coming from the stainless steel). Moreover, there is no evidence of oxygen inner migration in the matrix when forming the internal oxide products. However, Mn is slightly concentrated below the surface indicating the reaction with Cr to form spinel on the surface. This situation is quite different compared to the one after 24 h (EDS mapping in Fig. 5).

The external most layer is enriched with Mn, Cr and O, forming the spinel barrier $(Mn,Cr)_3O_4$, which is covering the Cr_2O_3 layer. Owing to the fast diffusion of Mn, this element diffuses through the chromia layer, and in response to the black band in the Mn mapping. 24 h at 950 ºC is enough to promote the internal migration of oxygen, generating internal oxides such as oxides with Ti and Al, and the intermetallic precipitate, which is enriched in Nb and Si.

EDS line scanning was conducted to further investigate the distribution of elements from the external oxide layer to the stainless steel matrix. The red line in Figure 3c corresponds to the analysis extension, and the results are presented in Fig. 6.

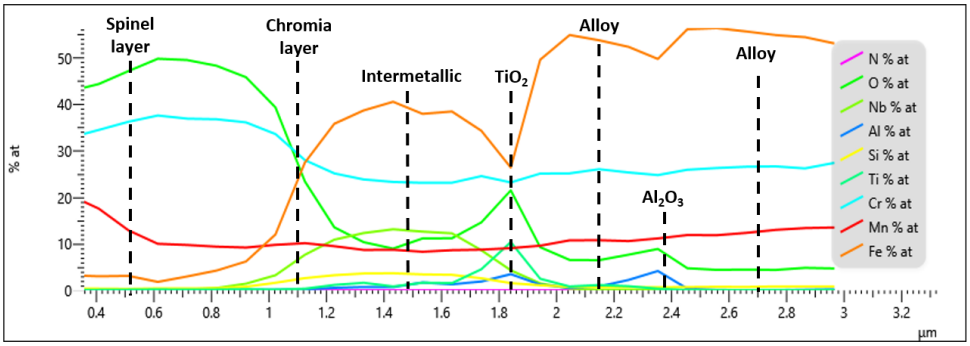

Figure 6. EDS line scanning of a ferritic stainless steel oxidised 24 h at 950 ºC, see also Fig. 3c.

This analysis identifies the species present in the oxide scale, which is formed with an external Cr-Mn spinel layer over an internal layer of Cr_2O_3 corundum layer with a total thickness of 1.1 µm. The presence of internal oxides under the interphase suggest that the internal oxygen diffusion occurs, generating internal oxides rich in Ti and Al in the stainless steel matrix. According to other authors, the intermetallic phases are mainly Fe, Nb and Si, and can precipitate within the ferritic bulk [12, 13].

2.5. Surface modification with platinum deposition

The oxidation of the ferritic stainless steel EN 1.4509 is a surface reaction that generates spinels on the surface. The deposition of species in the stainless steel substrate modifies the oxidation products. A platinum thin film was deposited by sputtering with a plasma coating system in a stainless steel EN 1.4509, which was immediately thermally treated at 950 ºC during 24 hours. The figures below present the oxides formed at 950 ºC for 24 hours between a platinum sputtered and non sputtered samples.

The influence of platinum deposition can be seen by comparing Figs. 7a and 7b. After the thermal treatment, the strongly modification can be seen even at low magnification. In the micrograph, it is possible to identify the shape of the crystals formed in the modified specimen, which is in contrast with the uncoated sample. It seems that the growth of the spinel is stimulated by platinum.

The magnified images of Fig. 7a is presented in Fig. 8. Apart from the large crystal size growth of the spinels, platinum promotes the formation of another crystal phase. As is showed in the micrographs, this new crystal grow with an hexagonal appearance. The EDS point analysis as shown in Table 2 reveals the formation of chromium oxide phase Cr_2O_3 (eskolaite).

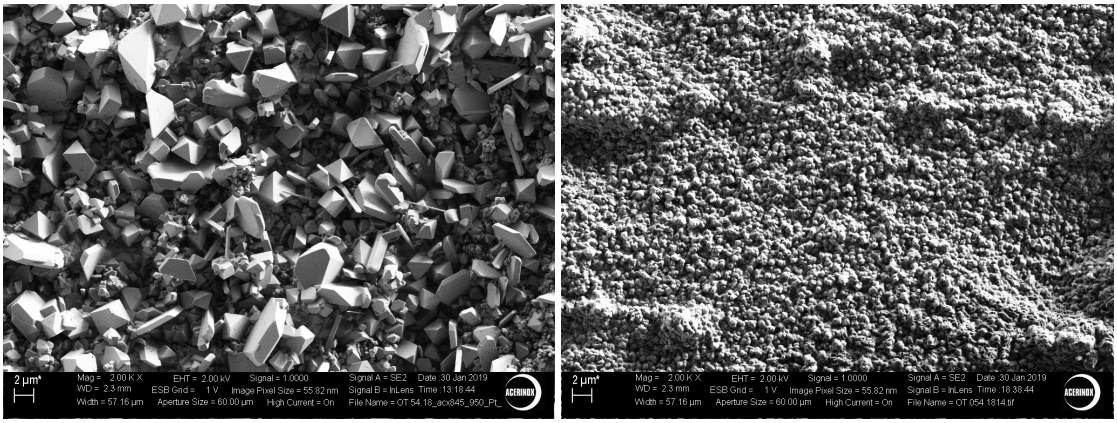

a) b)

Figure 7. Surface appearance of EN 1.4509 oxidised 24 h at 950 ºC. a) Pt-coating before thermal treatment. b) Uncoated.

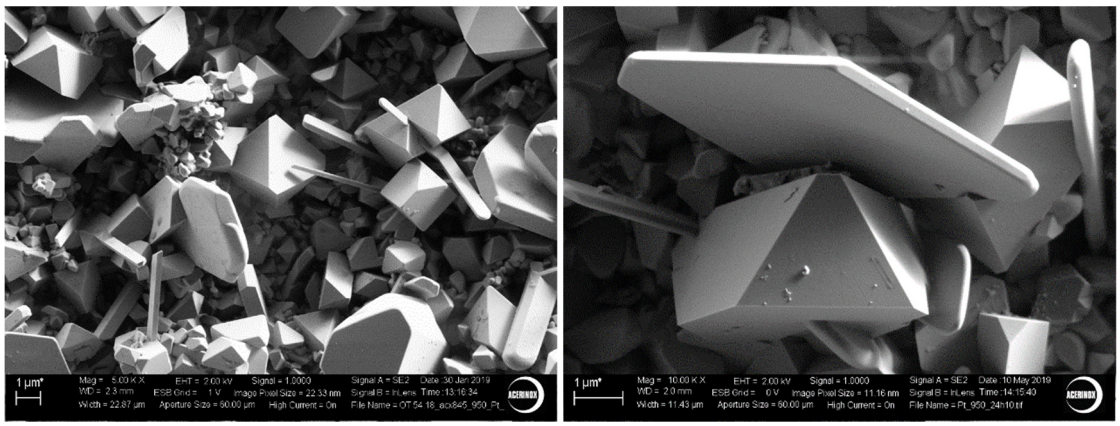

a) b)

Figure 8. SEM micrographs of the platinum deposited sample magnified at a) x5,000, and b) x10,000.

The deposition of platinum seems to modify the oxide scale growth mechanism. This alteration can also be observed in the cross-section as presented in Fig. 9. The cross-section of the Pt sputtered sample is shown in Fig. 9a, and reveals a thicker oxide scale than the unsputtered sample in Fig. 9b. Before the oxidation of the specimen, Pt was deposited as a thin film. However, after the thermal treatment, platinum is located in the oxide scale layer as a discrete metal shining inclusion (in BSE image mode). This behaviour was predicted by Stringer in 1966 [14]. The size of these particles was measured and can be found in a range between 25 nm to 170 nm.

In order to confirm that platinum is located as shining particles inside the oxide scale in Fig. 9A, an EDS mapping analysis in the cross-section of the specimen is shown in Fig. 10.

The results confirm that platinum is present inside the oxide scale forming discrete particles. The elemental distribution is similar to the uncoated samples; the signals for Cr, Mn and O are more intense. Another notable difference can be appreciated in the high concentration of internal oxides rich in Ti and Al. Furthermore, Si is present in the interphase oxide scale/metal bulk, forming a continuous barrier.

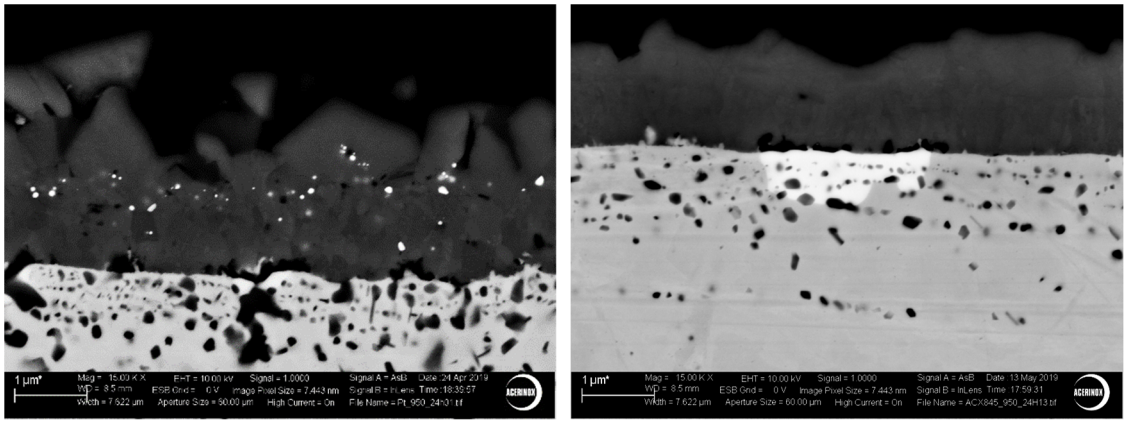

a) b)

Figure 9. Cross-section of EN 1.4509 oxidised 24 h at 950 ºC. a) Sputtered Pt before thermal treatment. b) Non-sputtered.

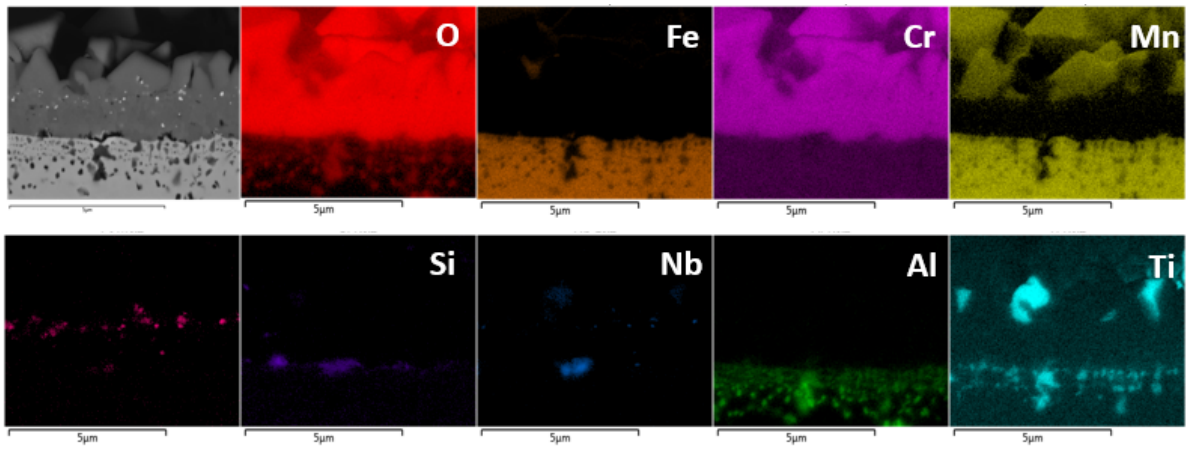

Figure 10. SEM-BSE cross-section micrographs and EDS mapping analysis over an oxidised Pt coated sample.

3. Conclusions

The oxidation of a commercial ferritic stainless steel EN 1.4509 was investigated over isothermal conditions at 950 ºC in air for different exposure times. The mass gained is increased with the exposure time and the kinetic law obeys the parabolic behaviour for 12 hours. This tendency is typical from protective oxide scale growth.

All the investigated samples exhibited an external Mn-Cr spinel layer over a chromium layer. However, the thickness of the oxide scale and the spinel size increase with the exposure time.

The oxide scales are formed by the outward migration of metallic elements from the ferritic alloy and the inward migration of the oxygen from the atmosphere. The EDS mapping analysis gives the distribution and the chemical composition of the involved elements in the oxidation process.

- The external diffusion of metallics elements, such as Mn and Cr toward the surface, reveals the multilayer oxide scale nature, which is formed by the Mn-Cr spinel external layer that grows over the chromia protective layer. The Mn EDS elemental map reveals how this element reaches the surface through the chromia layer.
- The oxygen internal diffusion can be seen below the interphase oxide scale/stainless steel matrix, developing internal oxides rich in Al and Ti.

The sample modification provided by the sputtering of platinum makes a significant contribution in the oxidation process.

- The 24 hours period of thermal treatment on modified sample with platinum deposition, generate a larger crystal size compared with the obtained after 168 hours oxidation process.
- The evaluation of the cross-section shows how platinum takes part of the oxide scale, forming discrete metallic inclusions. The EDS mapping analysis confirm that the final position of the elements is inside the oxide scale, but not forming a continuous layer.

Platinum induces the growth of hexagonal crystals of Cr_2O_3 over the EN 1.4509 surface. These crystals are vertically oriented. This new phase generated is not observable in non-sputtered samples.

Acknowledgements
I would especially like to thank the European Microbeam Analysis Society for the invitation to the EMAS 2019 Workshop at the NTNU, Realfagbygget, Trondheim, Norway. This research has been done during the second year of myPhD-thesis; therefore, I would like to thank the University of Seville the thesis programme "Science and Technology of New Materials". Pablo Navarro acknowledges to Acerinox Europa S.A.U. and also to the Spanish Ministry of Economy and Business for the financial support. This work is included in FERRINOP Project, co funded by CDTI (www.cdti.es).

References

[1] Roh H S, Koo K Y, Jung U H and Yoon W L 2017 Hydrogen production from natural gas steam reforming over Ni catalysts supported on metal substrates. *Curr. Appl. Phys.* **10** S37-S39
[2] Laguna O H, Domínguez M I, Centeno M A and Odriozola J A 2016 Forced deactivation and postmortemcharacterization of a metallic microchannel reactor employed for the preferential oxidation of CO (PROX). *Chem. Engng. J.* **30**2 650-662
[3] Sequeira C A C 2019 *High temperature corrosion: Fundamentals and engineering*. (Hoboken, NY: John Wiley and Sons) chapter 1, 35
[4] Wagner C 1936 *Z. Phys. Chem.* **32** 447
[5] Wei L, Zheng J, Chen L and Misra R D K 2018 High temperature oxidation behavior of ferritic stainless steel containing W and Ce. *Corrosion Sci.* **142** 79-92
[6] Khanna A 2012 High temperature oxidation. in: *Handbook of environmental degradation of materials*. (Kutz M; Ed.) (Norwich, NY: William Andrew Publishing) chapter 5, 127-194
[7] Stringer J, Wilcox B A and Jaffe R I 1972 The high-temperature oxidation of nickel-20 wt.% chromium alloys containing dispersed oxide phases. *Oxidation Metals* **1** 11-47
[8] Hosseini S N, Karimzadeh F, Enayati M H and Sammes N M 2016 Oxidation and electrical behavior of CuFe2O4 spinel coated Crofer 22 APU stainless steel for SOFC interconnect application. *Solid State Ionic* **289** 95-105
[9] Holcomb G and Alman D 2006 The effect of manganese additions on the reactive evaporation of chromium in Ni–Cr alloys. *Scripta Materialia* **54** 1821-1825
[10] Wei L, Han L, Chen L and Zhao Y 2018 Oxidation behaviour of cerium and tungsten-containing ferritic stainless steels at 1200 ºC in air. *Proc. Manuf.* **15** 1588-1595
[11] Col A, Parry V and Pascal C 2017 Oxidation of a Fe–18Cr–8Ni austenitic stainless steel at 850 °C in O2: Microstructure evolution during breakaway oxidation. *Corrosion Sci.* **114** 17-27
[12] Palcut M, Mikkelsen L, Neufeld K, Chen M, Knibbe R and Hendriksen P V 2010 Corrosion stability of ferritic stainless steels for solid oxide electrolyser cell interconnects. *Corrosion Sci.* **10** 3309-3320
[13] Alnegren P, Sattari M, Froitzheim J and Svensson J E 2016 Degradation of ferritic stainless steels under conditions used for solid oxide fuel cells and electrolyzers at varying oxygen pressures. *Corrosion Sci.* **110** 200-212
[14] Stringer J 1966 The effect of alloying on oxidation: Quantitative treatments. *Metall. Rev.* **11** 113-128